

# Transition radiation as a source of quasi-monochromatic X-rays

V. N. Baier and V. M. Katkov

Budker Institute of Nuclear Physics, 630090 Novosibirsk, Russia

## Abstract

Transition radiation (TR) from ultrarelativistic particles is considered. It is shown that performing collimation of the TR from the periodic N-foil stack (parameters of which are selected in a appropriate manner) one obtains the spectrum of the TR which has a form of a peak position of which  $\omega_1$  depends on the plasma frequency and the thickness of the radiator foils. The height and width of the peak depend on the collimation angle  $\vartheta_c$ . The height of the peak for given  $\vartheta_c$  is proportional to N. Selecting parameters one can have the source of X-rays of desired frequency with rather good monochromaticity.

# 1 Introduction

The transition radiation arises at uniform and rectilinear motion of a charged particle when it intersects a boundary of two different media (in general case, when it moving in a nonuniform medium or near such medium). This phenomenon [1] was actively investigated during a few last decades (see, e.g. reviews [2], [3]) and widely used in transition radiation detectors (see, e.g. recent review [4] and references therein).

We consider the standard TR radiator of  $N$  foils of thickness  $l_1$  separated by distances  $l_2$  in a gas or the vacuum, so the period length is  $l = l_1 + l_2$ . The plasma frequency of the foil and gap material are  $\omega_0$  and  $\omega_{02}$ , we neglect  $\omega_{02}$ . The basic features of the TR in this radiator depend essentially on the interrelation between values of  $\omega_1 = \frac{\omega_0^2 l_1}{4\pi}$  and  $\bar{\omega}_p = \omega_0 \gamma \sqrt{\frac{l_1}{l}}$ ,  $\gamma$  is the Lorentz factor. In the TR detectors the inequality  $\omega_1 \gg \bar{\omega}_p$  is fulfilled, in the usual case  $l_1 \ll l_2$  and radiated frequencies  $\omega < \omega_0 \gamma$ . The total energy radiated is proportional to  $\gamma$  and the TR detector are just used to measure this quantity.

In the opposite case  $\omega_1 \ll \bar{\omega}_p$  and  $l_1 \sim l_2$  characteristics of the TR are quite different. The total radiated energy is independent of  $\gamma$ . Performing the collimation of the radiation within angle  $\vartheta_c$  with respect velocity of the initial particle one can obtain the radiation concentrated in a rather narrow spectral band near  $\omega_1$ . The width of this band depend on  $\vartheta_c$ . There are limitations on the number of foils  $N$  due to absorption of the radiated X-rays and multiple scattering of the projectile. Nevertheless one can pick out parameters which permit obtain number of radiated per one crossing photons  $N_\gamma \sim 0.01 \div 1$  (per one projectile). This case is discussed in detail in Sec.2.

In Sec.3 the present situation with use of the TR as a X-ray source is discussed. Some specific features of the proposed radiator are analyzed including selection of the parameters. Set of examples of X-ray sources with various  $\omega_1$  utilizing distinct material of the foils and operating at different energies is collected in Table.

## 2 Transition radiation from the periodic N-foil stack

The spectral-angular distribution of emitted from ultrarelativistic electrons energy in the radiator consisting of many ( $N$ ) thin foils of the thickness  $l_1$  separated by equal distances  $l_2$  in a gas was discussed in many papers, see e.g. [3]-[7]

$$\frac{d^2\varepsilon}{d\omega dy} = \frac{4e^2 y}{\pi} \left( \frac{\kappa_0^2}{(1+y)(1+\kappa_0^2+y)} \right)^2 \sin^2 \frac{\varphi_1}{2} \frac{\sin^2(N\varphi/2)}{\sin^2(\varphi/2)}, \quad (1)$$

where  $\omega$  is the frequency of radiation,  $y = \vartheta^2 \gamma^2$ ,  $\gamma = \epsilon/m$  is the Lorentz factor,  $\epsilon(m)$  is the energy (the mass) of the incident electron,  $\vartheta$  is the azimuthal angle of

emission with respect velocity of the incident electron (we assume normal incidence),  $\kappa_0 = \omega_p/\omega$ , here  $\omega_p = \omega_0\gamma$ ,  $\omega_0$  is the plasma frequency

$$\omega_0^2 = \frac{4\pi e^2 n_e}{m}, \quad \varphi_1 = \frac{\omega l_1}{2\gamma^2} (1 + \kappa_0^2 + y), \quad \varphi_2 = \frac{\omega l_2}{2\gamma^2} (1 + y), \quad \varphi = \varphi_1 + \varphi_2, \quad (2)$$

where  $n_e$  is the density of electrons in the medium of a foil. The radiated energy is the coherent sum of the TR amplitudes for each interface and in absence of absorption Eq.(1) has the pronounced interference pattern.

Although the formula (1) is derived in classical electrodynamics, one can introduce the probability of the TR

$$\frac{d^2 w}{d\omega dy} = \frac{1}{\omega} \frac{d^2 \varepsilon}{d\omega dy} \quad (3)$$

In this paper the system  $\hbar = c = 1$  is used,  $e^2 = \alpha = 1/137$ . Recently authors developed the quantum theory of the TR and of the transition pair creation [8].

At  $N \gg 1$  the main contribution into the integral over  $y$  in (1), which defines the spectral distribution of the TR, gives the interval of  $\varphi$  for which

$$\sin^2 \varphi/2 \ll 1, \quad \varphi = 2\pi n + \Delta\varphi, \quad \Delta\varphi \sim \frac{1}{N}, \quad \Delta y \sim \frac{1}{N} \frac{2\gamma^2}{\omega l} = \frac{1}{N} \frac{l_c}{l}, \quad (4)$$

where  $l_c = 2\gamma^2/\omega$  is the formation length of radiation in the vacuum,  $l = l_1 + l_2$ . The condition

$$\varphi = \varphi_1 + \varphi_2 = \frac{\omega l}{2\gamma^2} (1 + y) + \frac{\omega l_1}{2\gamma^2} \kappa_0^2 = 2\pi n \quad (5)$$

defines the radiated photon energy  $\omega$  as a function of the emission angle  $\vartheta$  for fixed  $n$  (or for the  $n$ -th radiation harmonic  $\omega_n$ ). Respectively, the integral over  $y$  in (1) can be presented as a sum of the harmonic. We present (5) in a form

$$1 + y = \frac{l_1}{l} \left( \frac{\omega_p}{\omega_n} \right)^2 \left( 1 - \frac{\omega_n}{\omega} \right) \frac{\omega_n}{\omega} = \frac{\overline{\omega_p^2}}{\omega_n^2} \left( 1 - \frac{\omega_n}{\omega} \right) \frac{\omega_n}{\omega}, \quad (6)$$

where

$$\omega_n = \frac{\omega_1}{n}, \quad \omega_1 = \frac{\omega_0^2 l_1}{4\pi}, \quad \overline{\omega_p^2} = \gamma^2 \overline{\omega_0^2} = \gamma^2 \omega_0^2 \frac{l_1}{l}.$$

In practice it is convenient to use

$$\omega_1(eV) = 0.40344 \omega_0^2(eV) l_1(\mu m),$$

where the values  $\omega_1, \omega_0$  are expressed in  $eV$  and the value  $l_1$  is in  $\mu m$ .

Interrelation between values of  $\omega_1$  and  $\overline{\omega_p}$  ( $\overline{\omega_p} = (\overline{\omega_p^2})^{1/2}$ ) is very essential for the basic features of the TR. Consider first the case  $\omega_1 \gg \overline{\omega_p}$ . For this case the equation (5) has solutions for large  $n > 2\omega_1/\overline{\omega_p}$  only. In this situation the function

$$\sin^2 \frac{\varphi_1}{2} = \sin^2 \frac{\varphi_2}{2} = \sin^2 \left[ n\pi \frac{l_2}{l} \left( 1 - \frac{\omega_n}{\omega} \right) \right] \quad (7)$$

oscillates very fast and one can substitute it by the mean value equal to 1/2. In the integral over  $y$  in (1) represented as the sum of harmonic for large  $n$  one can substitute summation over  $n$  by integration

$$\int_0^\infty d(\Delta n) \frac{\sin^2(N\pi(\Delta n)/2)}{\sin^2(\pi(\Delta n)/2)} \simeq \frac{2}{\pi} \int_0^\infty \frac{dx}{x^2} \sin^2(Nx) = N \quad (8)$$

After this operation the variables  $y$  and  $\omega$  in (1) become independent. This means together with (8) that in this case the TR is the noncoherent sum of the single-interface contributions (the total number of interfaces is  $2N$ ). Actually just this case ( $\omega_1 \gg \overline{\omega_p}$ ) is used in the TR detectors, where the radiated energy is

$$E = \frac{2N}{3} \alpha \omega_0 \gamma \quad (9)$$

In the present paper we consider the opposite case  $\omega_1 \ll \overline{\omega_p}$ . In this case the characteristic angles of radiation are large comparing with  $1/\gamma$  (except boundaries of spectra for the given harmonic). These angles are defined by Eq.(6)

$$y_n \simeq \frac{\overline{\omega_p^2}}{\omega_n^2} \left(1 - \frac{\omega_n}{\omega}\right) \frac{\omega_n}{\omega}, \quad y_n^{max} = \frac{1}{4} n^2 a, \quad a = \frac{\overline{\omega_p^2}}{\omega_1^2} \gg 1. \quad (10)$$

If one performs collimation of the emitted radiation with the collimation angle  $y_c = \vartheta_c^2 \gamma^2 < y_n^{max}$  the frequency interval for the  $n$ -th harmonic is split into two parts:  $\omega_n \leq \omega \leq \omega_n^{(1)}$ ,  $\omega \geq \omega_n^{(2)}$ , where  $\omega_n^{(1,2)}$  are defined by equations following from (10)

$$\frac{\omega_n}{\omega_n^{(1,2)}} = \frac{1}{2} \left(1 \pm \sqrt{1 - z_n}\right), \quad z_n = \frac{y_c}{y_n^{max}} = \frac{4y_c}{n^2 a} = \frac{l}{l_1} \left(\frac{2\vartheta_c \omega_1}{n\omega_0}\right)^2, \quad (11)$$

where  $\omega_1$  is defined in (6). When the collimation is strong ( $y_c \ll y_1^{max} = a/4$ ) the radiation is concentrated in a rather narrow frequency band

$$\begin{aligned} \Delta\omega_n^{(1)} &= \omega_n^{(1)} - \omega_n \simeq \omega_n \frac{z_n}{4} = \omega_n \frac{y_c}{n^2 a} = \omega_1 \frac{y_c}{n^3 a}, \\ \omega_n^{(2)} &= \frac{4\omega_n}{z_n} = \omega_n \frac{n^2 a}{y_c} = \omega_1 \frac{na}{y_c}, \quad \frac{y_c}{a} = \frac{l}{l_1} \frac{\vartheta_c^2 \omega_1^2}{\omega_0^2}. \end{aligned} \quad (12)$$

The spectral distribution of the radiated energy on the  $n$ -th harmonic we obtain integrating Eq.(1) over  $y$  at  $N \gg 1$  in the interval near  $y$  satisfying the equation  $\varphi(y) = 2\pi n$

$$\int \frac{\sin^2(N\Delta\varphi/2)}{\sin^2(\Delta\varphi/2)} dy \simeq \frac{4\gamma^2}{\omega l} \int_{-\infty}^{\infty} \frac{\sin^2(Nx)}{x^2} dx = \frac{4\gamma^2}{\omega l} N\pi. \quad (13)$$

As it was indicated above, the relative width of the integration interval  $\Delta y/y \sim 1/N$  and within this accuracy at  $N \gg 1$  one can use the formula

$$\frac{\sin^2(N\varphi/2)}{\sin^2(\varphi/2)} \simeq \sum_{n=1}^{\infty} 2\pi N \delta(\varphi - 2\pi n). \quad (14)$$

This formula is exact at  $N \rightarrow \infty$ .

There is some analogy between radiation considered in this paper and the undulator radiation (see, e. g. [9]). In undulator the deviation of the particle's velocity  $\mathbf{v}$  from its mean value varies periodically under influence of the periodical (in space) magnetic field. In the considered case such deviation occurs with the wave vector  $\mathbf{k}$  of emitted radiation (the refraction index) while the particle's velocity remains constant. However, since the velocity  $\mathbf{v}$  and the wave vector  $\mathbf{k}$  are contained in expressions describing the radiation in the combination

$$1 - \mathbf{n}\mathbf{v} \simeq \frac{1}{2} \left( \frac{1}{\gamma^2} + \vartheta^2 + v_{\perp}^2 + \frac{\omega_0^2}{\omega^2} \right), \quad \mathbf{n} = \frac{\mathbf{k}}{\omega}, \quad (15)$$

the both effects are formally equivalent with respect to the coherence of radiation from different periods. The essential difference between considered the TR and the undulator radiation is due to the dependence of Eq.(15) on  $\omega$ . This property leads to the following consequences:

1. the characteristic frequencies of the undulator radiation are directly proportional to  $n$  (in contrast to  $\omega_n$  Eq.(6)) and inversely proportional to the structure period;
2. in the case considered for fixed  $n$  there is the maximal angle of radiation at  $\omega = 2\omega_n$  and for smaller angles  $\vartheta < \vartheta_m$  the interval of the allowed frequencies ( $\omega \geq \omega_n$ ) is divided into two intervals, which are larger than  $\omega_n$  in contrast to the undulator case.

Substituting Eqs.(14) and (6) into (3) we obtain for the spectral distribution of probability of radiation

$$\begin{aligned} \frac{dw}{d\omega}(y \leq y_c) &= \sum_{n=1}^{\infty} \frac{dw_n^c}{d\omega}, \quad \frac{dw_n^c}{d\omega} = \frac{4\alpha N}{\pi n} \\ &\times \frac{\sin^2 \left[ n\pi \frac{l_2}{l} \left( 1 - \frac{\omega_n}{\omega} \right) \right]}{(\omega - \omega_n) \left[ 1 + \frac{l_1}{l} \left( \frac{\omega}{\omega_n} - 1 \right) \right]^2} \vartheta(\omega - \omega_n) \left[ \vartheta(\omega_n^{(1)} - \omega) + \vartheta(\omega - \omega_n^{(2)}) \right], \quad (16) \end{aligned}$$

where  $\vartheta(x)$  is the Heaviside step function. Here the threshold values  $\omega_n^{(1,2)}$  are defined in Eq.(11), the value  $y_c$  is defined by the collimation angle ( $\vartheta_c = \sqrt{y_c}/\gamma$ ). Note that Eq.(16) is independent of the energy of particle. However, the condition of applicability this equation depends essentially on the Lorentz factor  $\gamma$ :

$$\omega_1 = \frac{\omega_0^2 l_1}{4\pi} \ll \bar{\omega}_p = \gamma \sqrt{\frac{l_1}{l}} \omega_0, \quad \gamma \gg \frac{\omega_0 \sqrt{l_1 l}}{4\pi} \quad (17)$$

The formula (16) was obtained in absence of X-ray absorption which is especially essential in the low frequency region. Taking into account absorption we find limitation on the number of foils  $N \sim N_{ef}(\omega)$  and

$$N_{ef}(\omega) = \frac{1}{\sigma(\omega)l_1} (1 - \exp(-N\sigma(\omega)l_1)), \quad (18)$$

where  $1/\sigma(\omega)$  is the X-ray attenuation length at the frequency  $\omega$ . We assume that the absorption in a single foil is small.

For the strong collimation ( $y_c \ll a/4$ ) the spectral probability of radiation on the  $n$ -th harmonic can be written as

$$\begin{aligned} \frac{dw_{n1}^c}{d\omega} &\simeq \frac{4\alpha N\pi n^3 l_2^2}{\omega_1^2 l^2} \left( \omega - \frac{\omega_1}{n} \right), \quad \omega - \frac{\omega_1}{n} \geq 0, \quad \omega - \frac{\omega_1}{n} \leq \frac{\omega_1 y_c}{n^3 a}; \\ \frac{dw_{n2}^c}{d\omega} &\simeq \frac{4\alpha N\omega_1^2 l^2}{\pi n^3 \omega^3 l_1^2} \sin^2 \left( \pi n \frac{l_1}{l} \right), \quad \omega \geq n\omega_1 \frac{a}{y_c}. \end{aligned} \quad (19)$$

These probabilities attain the maximal values on the boundaries of the regions. These values are

$$\frac{dw_{n1}^c}{d\omega} \left( \omega = \omega_n^{(1)} \right) = \frac{4\alpha N\pi l_2^2 y_c}{\omega_1 l^2 a}, \quad \frac{dw_{n2}^c}{d\omega} \left( \omega = \omega_n^{(2)} \right) = \frac{4\alpha N l^2}{\pi \omega_1 n^6 l_1^2} \left( \frac{y_c}{a} \right)^3 \sin^2 \left( \pi n \frac{l_1}{l} \right). \quad (20)$$

Integrating (19) over  $\omega$  we obtain the total number of the passing through the collimator photons:

$$w_{n1}^c = 2\alpha N\pi \frac{1}{n^3} \left( \frac{l_2}{l} \right)^2 \left( \frac{y_c}{a} \right)^2, \quad w_{n2}^c = \frac{2\alpha N}{\pi n^5} \left( \frac{l}{l_1} \right)^2 \left( \frac{y_c}{a} \right)^2 \sin^2 \left( \pi n \frac{l_1}{l} \right). \quad (21)$$

The corresponding expressions for the energy losses due to collimated X-ray emission are

$$E_{n1}^c = 2\alpha N\pi \frac{\omega_1}{n^4} \left( \frac{l_2}{l} \right)^2 \left( \frac{\Delta\omega}{\omega_1} \right)^2, \quad E_{n2}^c = \frac{4\alpha N\omega_1 y_c}{\pi n^4 a} \left( \frac{l}{l_1} \right)^2 \sin^2 \left( \pi n \frac{l_1}{l} \right). \quad (22)$$

It is seen from these expressions that one can neglect the contribution of higher harmonics ( $n \geq 2$ ). The contribution of the first harmonic is concentrated in the narrow frequency interval  $\Delta\omega \sim \omega_1 y_c/a \ll \omega_1$  while in the second available interval the frequencies much larger than  $\omega_1$  contribute ( $\omega \sim \omega_1 a/y_c \gg \omega_1$ ). So, the collimated TR in the forward direction have quite good monochromaticity.

Note that side by side with absorption there is another process which imposes limitation on the number of foils  $N$  especially when the angle of collimation is small. This process is multiple scattering of the projectile which leads to a "smearing" of the  $\delta$ -function in Eq.(14) and thus reduces the degree of the monochromaticity. Below we discuss these both processes for some particular examples.

We estimate now the contribution of higher harmonics ( $n \gg 1$ ) into the spectral distribution of probability in absence of the collimation. For  $\omega \geq \omega_1$  this contribution is suppressed as  $1/n^3$ . For  $\omega \ll \omega_1$  the main contribution give values  $n \sim \omega_1/\omega \gg 1$ . In this situation the spectrum becomes quasicontinuous, the factor  $\sin^2(\varphi_1/2)$  in Eq.(1) is oscillating very fast and one can substitute it by  $1/2$ . The summation over  $n$  can be replaced by the integration and this is integration of  $\delta$ -function in (14). For integration over  $y$  the variables  $\omega$  and  $y$  can be considered as independent. Taking this into account and integrating (1) over interval  $\frac{4\gamma^2}{\omega l_2} \leq y$  ( $\frac{\varphi_2}{2} \geq 1$ ) we find

$$\frac{dw}{d\omega} (\omega \ll \omega_1) \simeq \frac{2\alpha N}{\pi\omega} \left[ \ln \left( \pi \frac{\omega_1 l_2}{\omega l_1} \right) + const \right] \quad (23)$$

### 3 Discussion

Use of the TR as a source of X-rays was investigated recently in many papers (see [7]-[14] and references cited therein). Starting from differential spectral-angular distribution of radiated energy Eq. (1) authors analyzed position of maxima in this distribution. The corresponding resonance conditions are

$$\frac{\varphi_1}{2} = (2m - 1)\frac{\pi}{2}, \quad \frac{\varphi}{2} = m'\pi, \quad m, m' = 1, 2, 3 \dots \quad (24)$$

When these conditions are fulfilled there is connection between the emission angle and the photon energy. Measurements were preformed for variety of energies using different foils and various  $N, l_1, l_2$ . Typically spectral X-ray intensity was measured as function of the emission angle for fixed photon energy or as function of the photon energy at fixed emission angle. Experimental results obtained in [7]-[14] are in quite good agreement with theoretical calculations.

In [13] yield of X-ray photons (with energy  $2 \div 6$  keV) from electrons with energy  $\epsilon = 855$  MeV was  $N_\gamma \sim 10^{-4}$  per electron and width of the spectral band was  $\Delta\omega \sim \omega$  for Kapton foils and  $N = 3$ . In [14] yield of X-ray photons from electrons with energy  $\epsilon = 900$  MeV (with energy 14.4 and 35.5 keV) was  $N_\gamma \sim 2 \cdot 10^{-5}$  and  $N_\gamma \sim 6 \cdot 10^{-5}$  per electron respectively and width of the spectral band (FWHM) was  $\Delta\omega = 0.5$  keV and  $\Delta\omega = 0.81$  keV for Silicon monocrystalline foils and  $N = 10$  and  $N = 100$ .

Now we turn to some specific features of proposed approach. The ratio of thicknesses  $l_1$  and  $l_2$  is the important characteristic of the TR radiator. The thickness  $l_1$  is defined by the radiation frequency (energy)  $\omega_1$  Eq.(6) which can be written in a form

$$\omega_1 = \alpha m n_e \lambda_c^2 l_1, \quad (25)$$

where  $n_e = Zn_a$  ( $n_a$  is density of atoms in the foil),  $n_e$  is defined in Eq.(2),  $\lambda_c = 1/m = (\hbar/mc)$  is the Compton wavelength. It is seen from Eq.(21) that the number of collimated photons increases with  $l_2$  (the factor  $(l_2/l)^2$ ). From the

other side, the inequality  $\overline{\omega_p} \gg \omega_1$ , which have to be fulfilled in our case, becomes more strong if  $l_1/l$  increases. In this situation the requirement on the collimation angle  $\vartheta_c$  becomes more weak and influence of the multiple scattering diminishes (for the given monochromaticity of the radiation):

$$\vartheta_c^2 = \frac{l_1 \omega_0^2 \Delta\omega_1}{l \omega_1^2 \omega_1} > \vartheta_s^2 = \frac{4\pi N l_1}{\alpha \gamma^2 L_{rad}}, \quad (26)$$

where  $L_{rad}$  is the radiation length. So, the optimal value of  $l_2$  should be of the same order as  $l_1$ . Note that in the TR detectors where  $\overline{\omega_p} \ll \omega_1$  there is no limitation connected with the multiple scattering and the thickness  $l_2$  usually one order of magnitude larger than  $l_1$ . From (26) we have the limitation on the value  $N$  due to multiple scattering

$$N < N_s = \frac{\alpha L_{rad} \overline{\omega_p^2} \Delta\omega_1}{4\pi l_1 \omega_1^2 \omega_1}. \quad (27)$$

Using the definitions  $\overline{\omega_p^2}$  and  $\omega_1^2$  (6) and explicit formula for  $L_{rad}$  (valid for large  $Z$ ) we rewrite (26) in the form

$$N_s = \frac{\gamma^2 l_1}{4l} \frac{n_a}{\omega_1^3 \ln(183Z^{-1/3})} \frac{\Delta\omega_1}{\omega_1}. \quad (28)$$

So  $N_s \propto \gamma^2$  and  $N_s \propto \omega_1^{-3}$  and increases when the energy  $\omega_1$  diminishes. For low  $\omega_1$  the photon absorption (see Eq.(18)) becomes essential. Since for  $\omega \leq 10$  keV the x-ray attenuation length  $1/\sigma(\omega)$  for the heavy elements is from two to three order of magnitude shorter than for the light elements, one can use in this region of  $\omega$  the light elements only. In the region  $\omega \geq 30$  keV the attenuation length is rather long, but for large  $\omega_1$  the influence of the multiple scattering of the projectile (28) becomes more essential. In this region one can provide enough large  $N_s$  having used the large Lorentz factor only. For hard X-ray the difference between use of the heavy elements or the light elements is not so significant.

We consider a few examples of the X-ray yield basing on the results obtained above. In Fig.1 the spectral distribution of the radiated energy  $\frac{d\varepsilon}{d\omega}$  Eq.(1) is shown for Li foils ( $\epsilon = 25$  GeV,  $l_1 = 0.13$  mm,  $l = 3l_1$ ,  $N = 100$ ). The important effect of the dependence of the width and form of the first harmonic peak ( $\omega_1 = \frac{\omega_0^2 l_1}{4\pi} = 10$  Kev) Eq.(6) on the collimation angle  $\vartheta_c$ , ( $y_c = \vartheta_c^2 \gamma^2$ ) is given. It is seen that the collimation is cutting out the different parts of the radiation spectrum. The connection between the frequency and the emission angle is the specific property of the undulator type radiation. When the collimation angle decreases the spectral peak becomes more narrow (correspondingly the total number of emitted photons decreases also) and vise versa. The curve 5 exhibits the situation when the value  $y_c$  is near the boundary value  $y_{max}$  Eq.(10). For the curve 6 one has  $y_c > y_{max}$  and the spectral curve is independent of the collimation angle. The position of the right slope of the peak  $\omega_n^{(1)}$  is defined from Eq.(11), e.g. for  $y_c = 250$  one has  $\omega_1^{(1)} = 12.6$  keV or  $\Delta\omega/\omega \simeq 0.25$ .



In Fig.2(a) the dependence of the height the  $\frac{d\varepsilon}{d\omega}$  Eq.(1) on the number of foils ( $N = 20, 100, 200$ ) for the fixed collimation angle ( $y_c = 250$ ) is presented. The width of the peak is practically independent of  $N$ , while the height is proportional to  $N$ . The peaks of higher harmonics are situated at  $\omega_n = \omega_1/n$  ( $n=2, 3, 4$ ). Their characteristics are: the height  $\propto 1/n$  and the width  $\propto 1/n^3$  (see Eqs.(19)-(21), it is necessary to remind that in Figs.1,2 the energy losses spectrum is shown, while these equations are for the probability spectrum). Note that spectra shown in Fig.2(a) are calculated without absorption. If one takes the absorption into account the higher harmonics will be strongly suppressed.

There is also the hard part of the emitted spectrum which is given in Fig.2(b). This is the contribution of the first harmonic (see Eqs.(20) and (21)). For  $y_c = 250$  the position of the left slope  $\omega_1^{(2)} \simeq 48$  keV (see Eq.(11)). As the collimation becomes more strong the value  $\omega_1^{(2)}$  increases. Note, that the absorption is much weaker for the hard part of the spectrum.

Calculating the area of the peak in Fig.1,2 one can estimate number of radiated photons per electron  $N_\gamma$ , for  $y_c = 250$  one has  $N_\gamma \sim 0.1$  for  $N=100$ . Number of foil  $N = 500 \div 1000$  is typical in many experiments with the TR detectors, the lithium foils were used in [15]. Quite good estimation of  $N_\gamma$  can be obtained using (21), if  $N < N_s$ , substituting  $N = N_{ef}$ . Because of limitations connected with the photon absorption and the multiple scattering of the projectile one have to use the light elements.

Although results given in Figs.1 and 2 are obtained for the particular substance and the definite parameters, these results are quite universal at least qualitatively.

There is an opportunity to install the proposed TR radiator in the electron storage ring. In this case the number  $N$  will be defined by the storage ring operational regime. Let us note that at  $N = 20$  the first harmonic peak is quite distinct.

The approach proposed in this paper permits to obtain the yield of X-ray photons  $N_\gamma \sim 0.01 \div 1$  per electron and the width of the spectral band up to  $\Delta\omega/\omega \sim 0.1$ . Of course, the yield decreases for a more narrow spectral band. This means at least two order of magnitude increase of the yield comparing with obtained in [14]-[15].

Some specific examples are given in Table where  $N_1 = \frac{1}{\sigma(\omega_1)l_1}$  defines the value  $N_{ef}$  for fixed  $N$  and  $\omega_1$  (18). The values  $N_s$  are calculated according with Eq.(27). If  $N_s > N_1$  we choose  $N$  slightly larger than  $N_1$ . In the opposite case we choose  $N$  slightly smaller than  $N_s$ . In the first column the material of the foil is given,  $\text{CH}_2$  is used for Polyethylene. The value  $N_\gamma$  is the number of photons emitted into collimator for the given values of  $\omega_1$  and  $\Delta\omega_1$ . All calculations are performed for  $l = 3l_1$ . The results in Table are in a reasonable agreement with Figs.1,2.

### Acknowledgments

This work was supported in part by the Russian Fund of Basic Research under Grant 98-02-17866.

## References

- [1] V. L. Ginzburg and I. M. Frank, J. Phys. USSR **9** (1945) 353.
- [2] V. L. Ginzburg and V. N. Tsytovich, Physics Reports **49** (1979) 1.
- [3] M. L. Ter-Mikaelian, *High Energy Electromagnetic Processes in Condensed Media*, John Wiley & Sons, 1972; Sect. 4.
- [4] B.Dolgoshein, Nucl.Instr. and Meth. **A 326** (1993) 434.
- [5] G. M. Garibyan, Sov.Phys.JETP **33** (1971) 23.
- [6] X.Artru, G.Yodh and G.Mennessier, Phys.Rev. **D 12** (1975) 1289.
- [7] M. L. Cherry, Phys.Rev. **D 17** (1978) 2245.
- [8] V.N.Baier and V.M.Katkov, hep-th 9811302, BINP preprint 98-82, 1998; Phys.Lett.A (to be published).
- [9] V.N.Baier, V.M.Katkov and V.M.Strakhovenko, *Electromagnetic Processes at High Energies in Oriented Single Crystals*, World Scientific Publishing Co, Singapore, 1998.
- [10] M. A. Piestrup, J. O. Kephart, H. Park et al., Phys.Rev. **A 32** (1985) 917.
- [11] M. A. Piestrup, D. G. Boyers, C. I. Pinkus et al., Phys.Rev. **A 45** (1992) 1183.
- [12] P.Goedtkindt, J.M.Salome, X.Artru et al., Nucl.Instr. and Meth. **B 56/57** (1991) 1060.
- [13] H.Backe, S.Gampert, A.Grendel et al., Z.Phys. **A 349** (1994) 87.
- [14] Y.Takashima, K.Aramitsu, I.Endo et al., Nucl.Instr. and Meth. **B 145** (1998) 25.
- [15] J. Cobb, C. W. Fabian, S.Iwata et al., Nucl.Instr. and Meth. **140** (1975) 413.

## Figure captions

- **Fig.1** The spectral distribution of the radiated energy  $E(\omega) \equiv \frac{d\varepsilon}{d\omega}$  Eq.(1) in units  $2\alpha/\pi$  vs photon energy for *Li* foils ( $\epsilon = 25$  GeV,  $l_1 = 0.13$  mm,  $l = 3l_1$ ,  $N = 100$ ). The dependence of the width and form of the first harmonic peak ( $\omega_1 = 10$  Kev) Eq.(6) on the collimation angle  $\vartheta_c$  is shown. This angle is measured in units  $y_c = \vartheta_c^2 \gamma^2$ :  $y_c = 150, 200, 250, 300, 350, 400$  for curves 1, 2, 3, 4, 5, 6 respectively.
- **Fig.2** The spectral distribution of the radiated energy  $E(\omega) \equiv \frac{d\varepsilon}{d\omega}$  Eq.(1) in units  $2\alpha/\pi$  vs photon energy for *Li* foils ( $\epsilon = 25$  GeV,  $l_1 = 0.13$  mm,  $l = 3l_1$ ,  $y_c = 250$ ). The dependence of the height of the spectral curve on the number of foils is presented ( $N = 20, 100, 200$  for curves 1, 2, 3 respectively).
  - **(a)** The soft part of the spectral curve. The main (the first harmonic) peak and peaks of  $n = 2, 3, 4$  harmonics ( $\omega_n = \omega_1/n$ ) are seen.
  - **(b)** The hard part of the spectral curve.

TABLE Characteristic parameters of the radiation process in the TR radiator

foil	$\omega_0$ (eV)	$l_1$ ( $\mu m$ )	$\omega_1$ (keV)	$N_1$	$\varepsilon$ (GeV)	$\frac{\Delta\omega_1}{\omega_1}$	$N_S$	$N$	$N_{ef}$	$N_\gamma \cdot 10^2$
Li	13.8	26	2	36	1	0.1	200	50	27	0.55
Li	13.8	39	3	74	1	0.2	120	100	55	4.5
Li	13.8	130	10	440	5	0.3	120	100	90	17
Li	13.8	130	10	440	25	0.3	3000	1000	400	72
Li	13.8	390	30	360	25	0.2	74	60	55	4.5
Li	13.8	650	50	240	25	0.3	24	20	20	3.7
CH <sub>2</sub>	20.9	57	10	110	5	0.2	140	120	73	6
CH <sub>2</sub>	20.9	57	10	110	25	0.1	1750	200	92	1.9
CH <sub>2</sub>	20.9	170	30	250	25	0.2	130	100	82	6.7
CH <sub>2</sub>	20.9	285	50	190	25	0.2	28	25	23	1.9
Si	31	77	30	39	25	0.2	130	80	34	2.8
Si	31	130	30	100	25	0.2	28	25	22	1.8

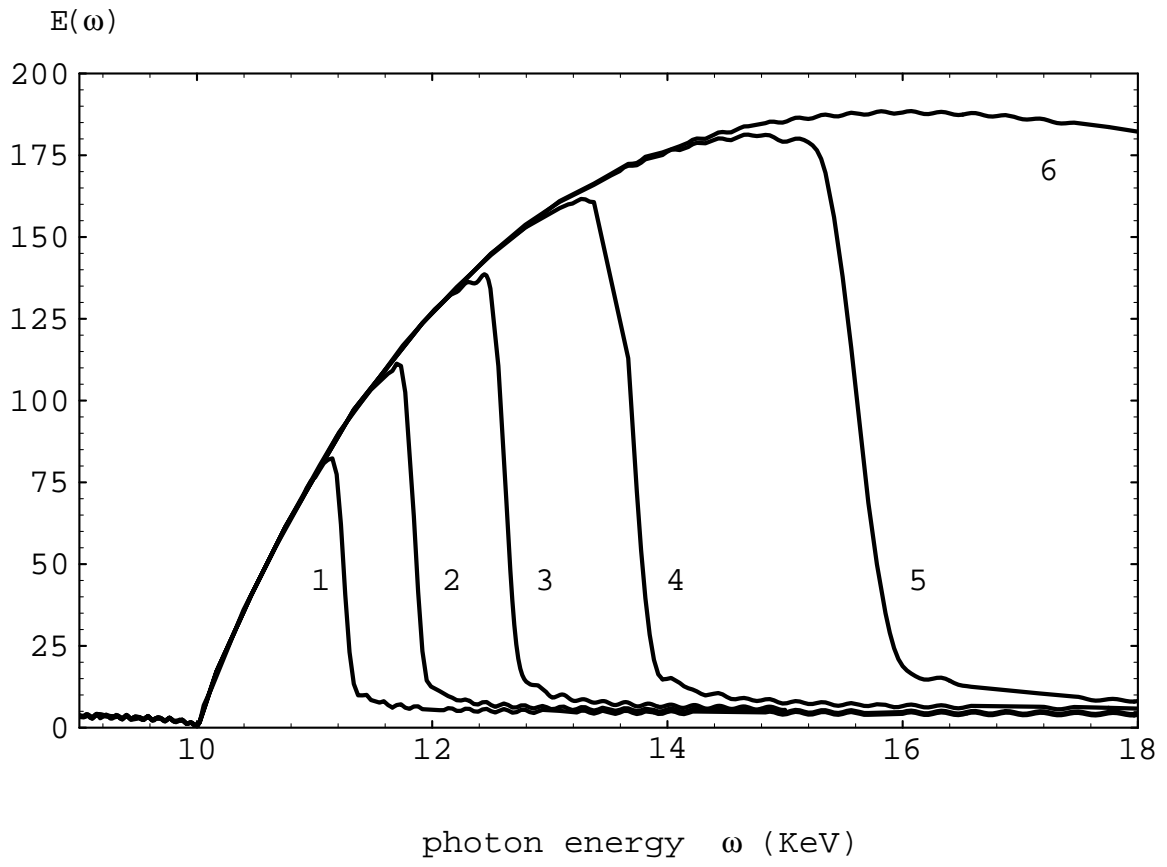


Fig.1

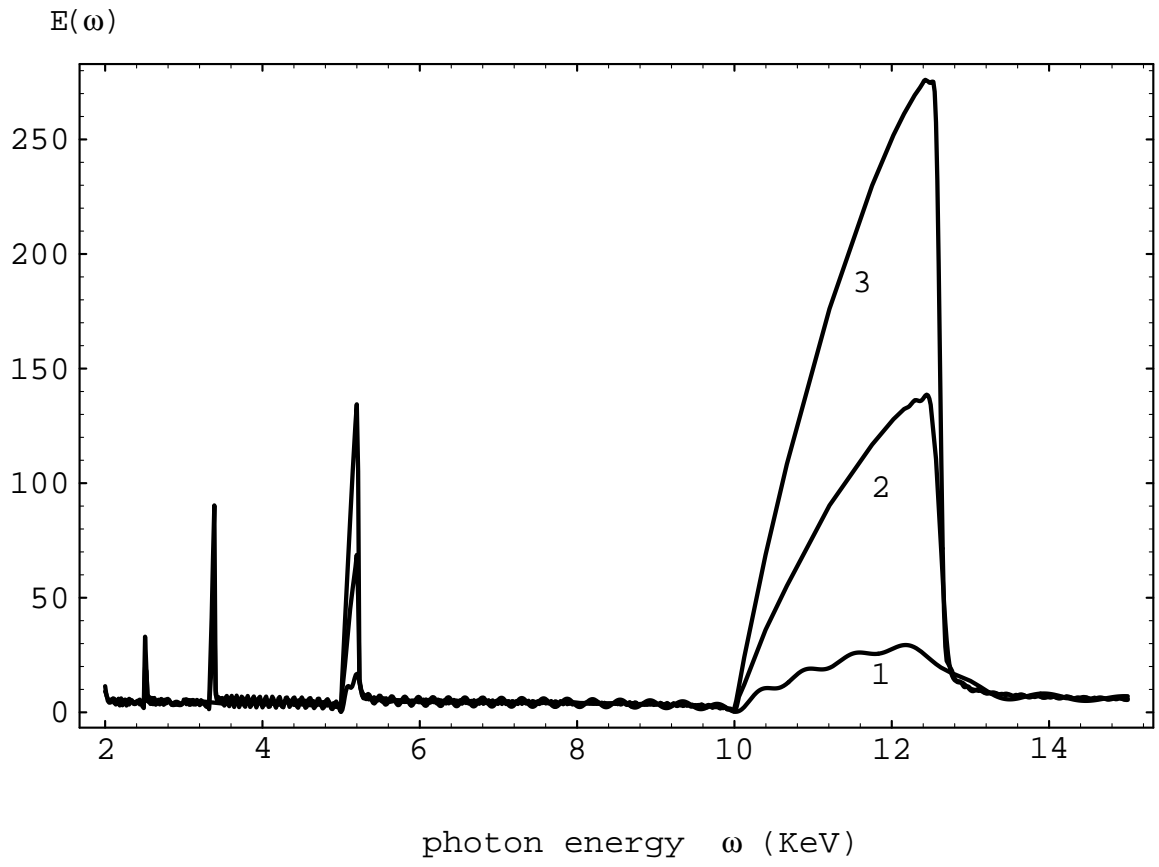


Fig.2

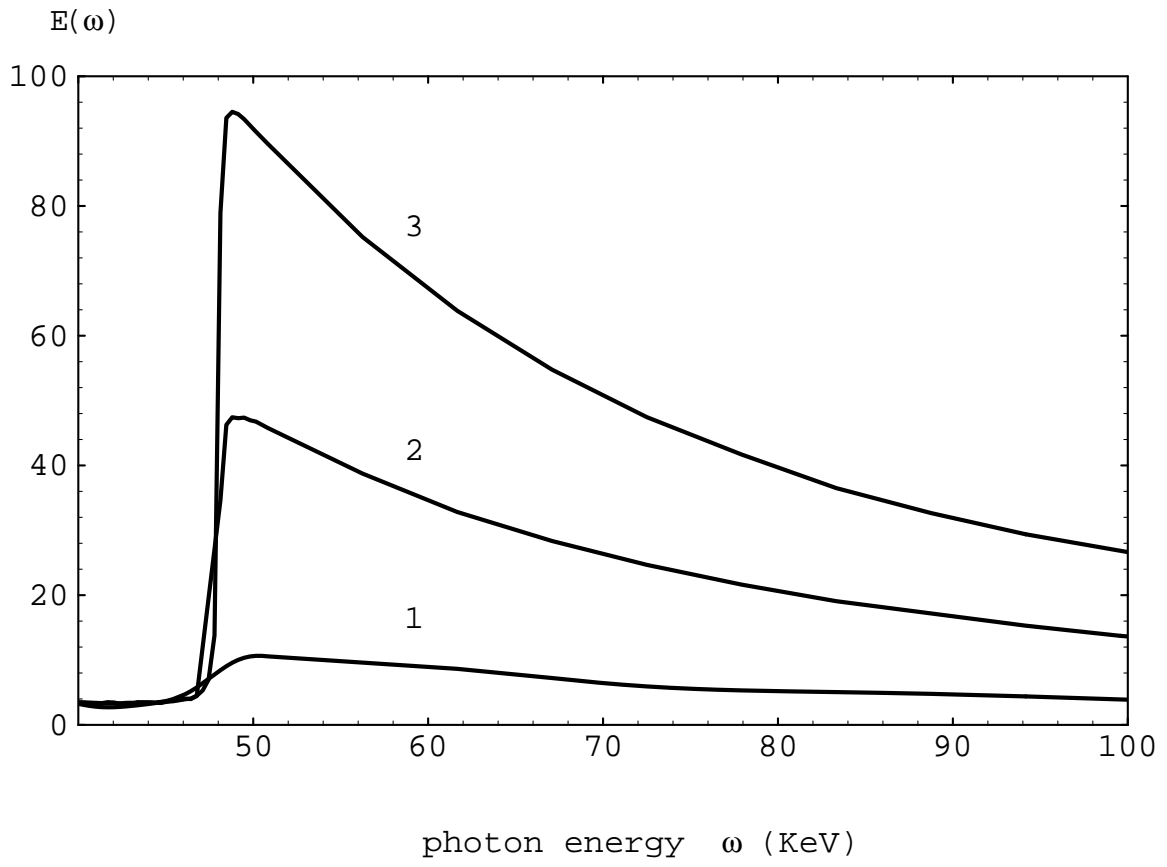


Fig.3